Supporting Information (SI) for

Fast and ultrasensitive glycoform analysis by supercritical fluid chromatography-tandem mass spectrometry

Yoshimi Haga[1], Masaki Yamada[2], Risa Fujii[1], Naomi Saichi[1], Takashi Yokokawa[3], Toshihiro Hama[3], Yoshihiro Hayakawa[2], and Koji Ueda[1*]

[1]Cancer Proteomics Group, Cancer Precision Medicine Center, Japanese Foundation for Cancer Research, 3-8-31 Ariake, Koto-ku, Tokyo 135-8550, Japan

[2]Global Application Development Center, Shimadzu Corporation, Nishinokyo Kuwabara-cho 1, Nakagyo-ku, Kyoto 604-8511, Japan

[3]Department of Pharmacy, Cancer Institute Hospital, Japanese Foundation for Cancer Research, 3-8-31 Ariake, Koto-ku, Tokyo 135-8550, Japan

*** Corresponding author:** Koji Ueda
E-mail: koji.ueda@jfcr.or.jp

This SI contains the following:

Figure S1

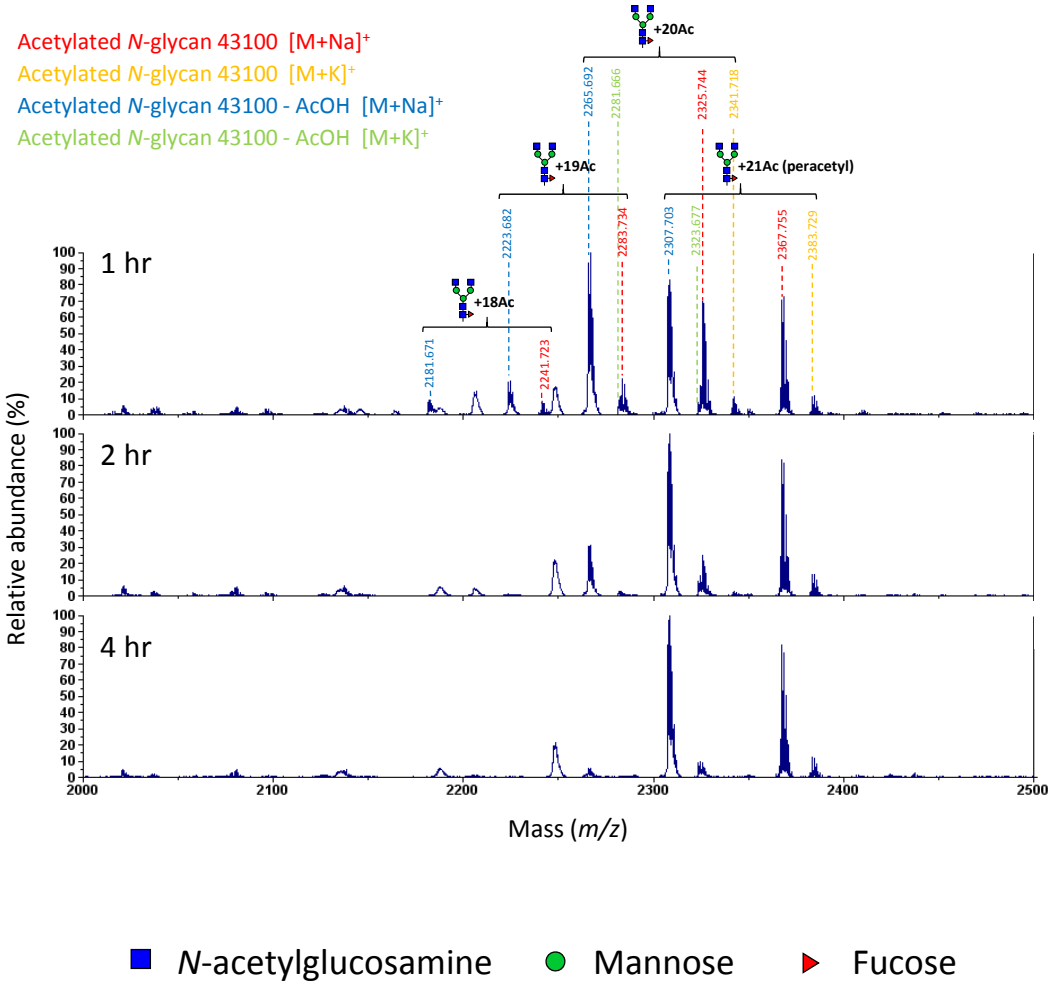

Figure S1. MALDI-TOF-MS spectrum of time course experiments under acetylation of N-glycans. The released N-glycans from Bevacizumab were acetylated at 50 °C for indicated time. De-acetic acid forms (blue and green) were MALDI-specific byproducts.

Figure S2

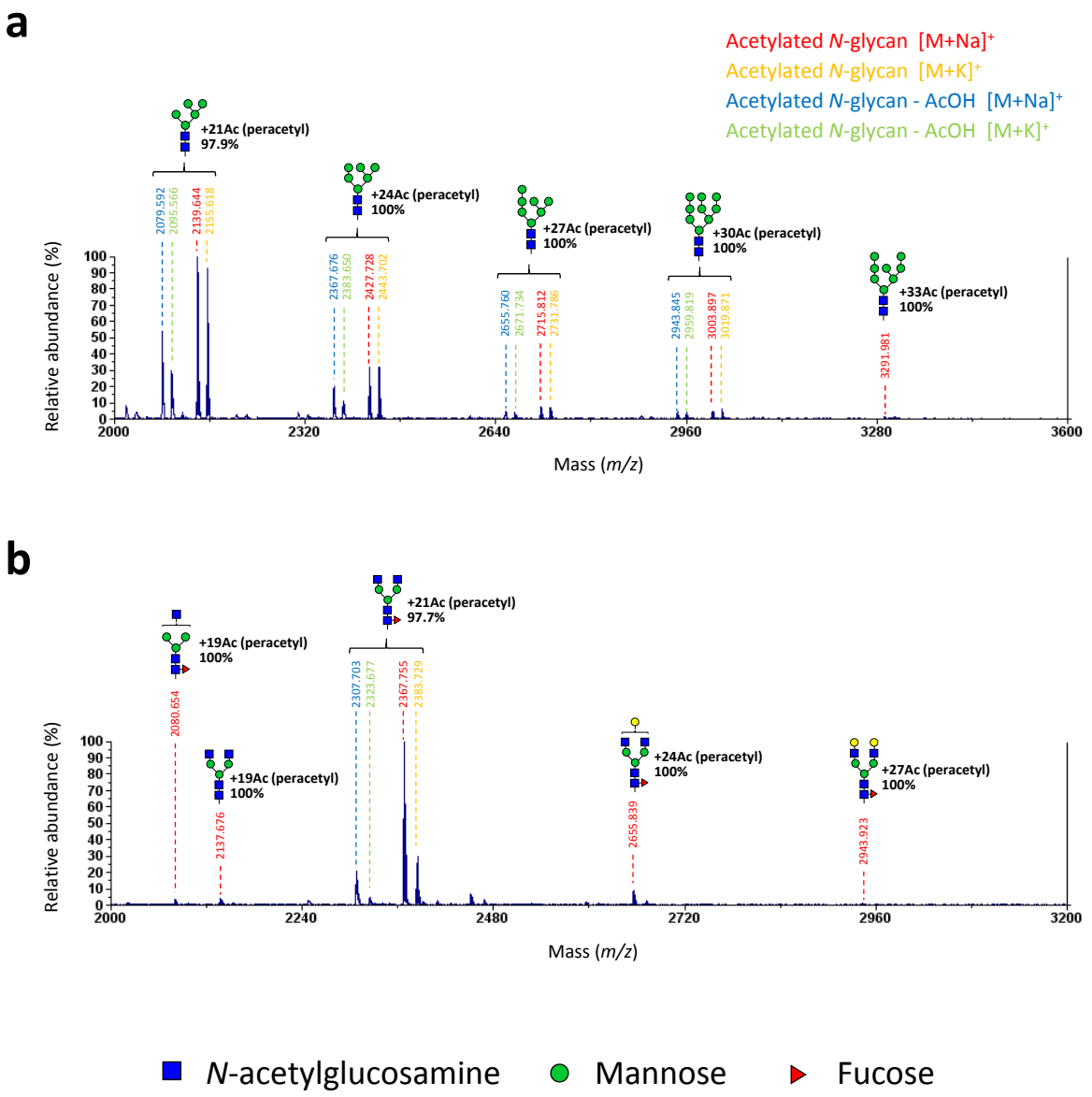

Figure S2. MALDI-TOF-MS spectrum of acetylated N-glycans. The released N-glycans from (a) RNase B and (b) Bevacizumab were acetylated at 50 °C for 4 hr. The percentages in the figure indicate the efficiency of labeling (i.e. peracetylation). De-acetic acid forms (blue and green) were MALDI-specific byproducts.

Figure S3

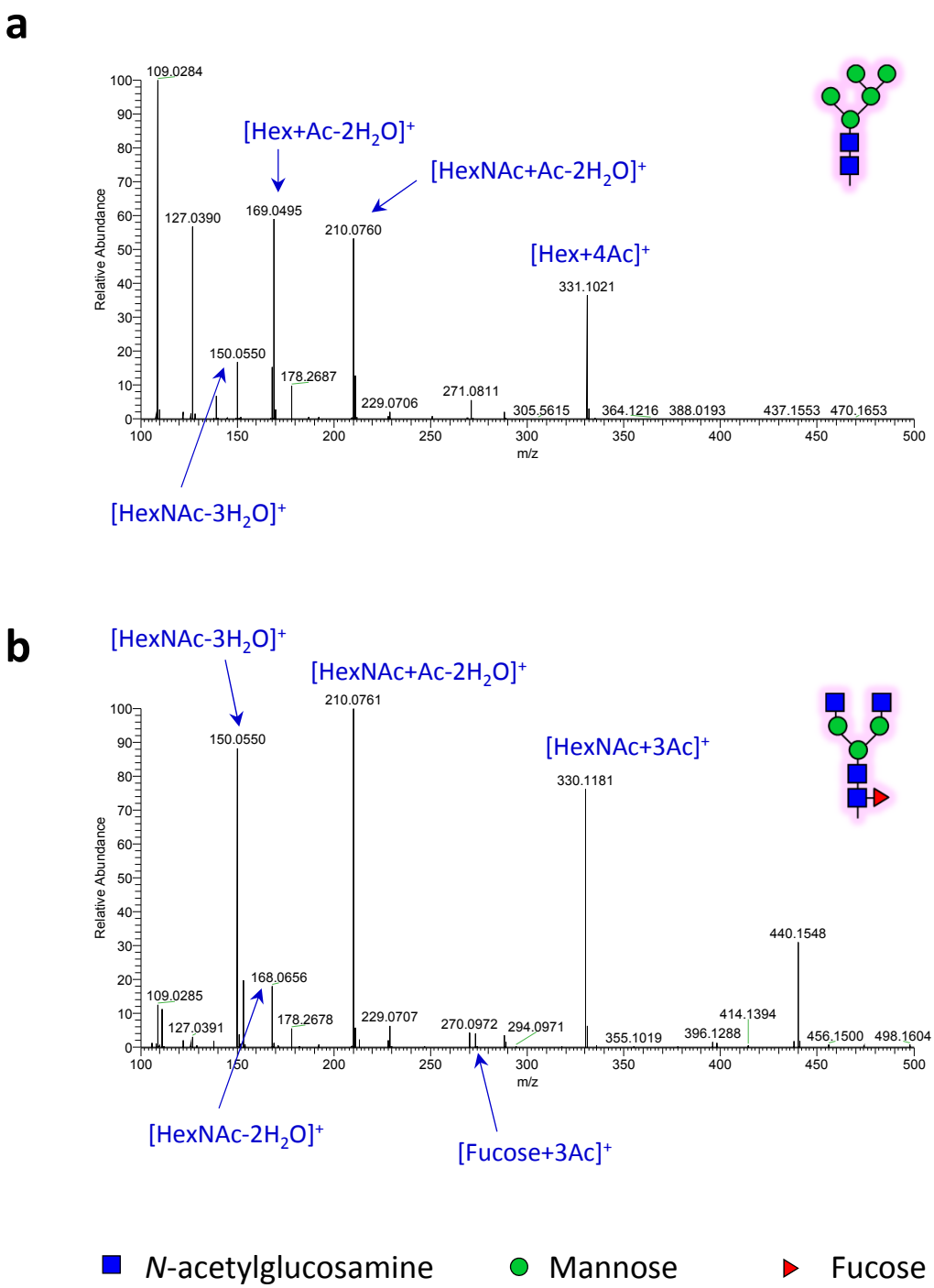

Figure S3. MS/MS fragmentation spectra of peracetylated N-glycans. Acetylated N-glycans were dissolved in methanol, directly infused and analyzed by Orbitrap Fusion Lumos (Thermo Fisher Scientific). Product ion spectrum of the $[M+H]^+$ ion at (a) m/z 2117.65 (Peracetylated Glycan 25000, prepared from RNase B), (b) m/z 2345.77 (Peracetylated Glycan 43100, prepared from bevacizumab).

Figure S4


25000
26000
27000
28000
29000
33000
33100
34100
35100
43000
43100
44000
Intensity
Collision energy, eV
150
210

Figure S4 (continued)

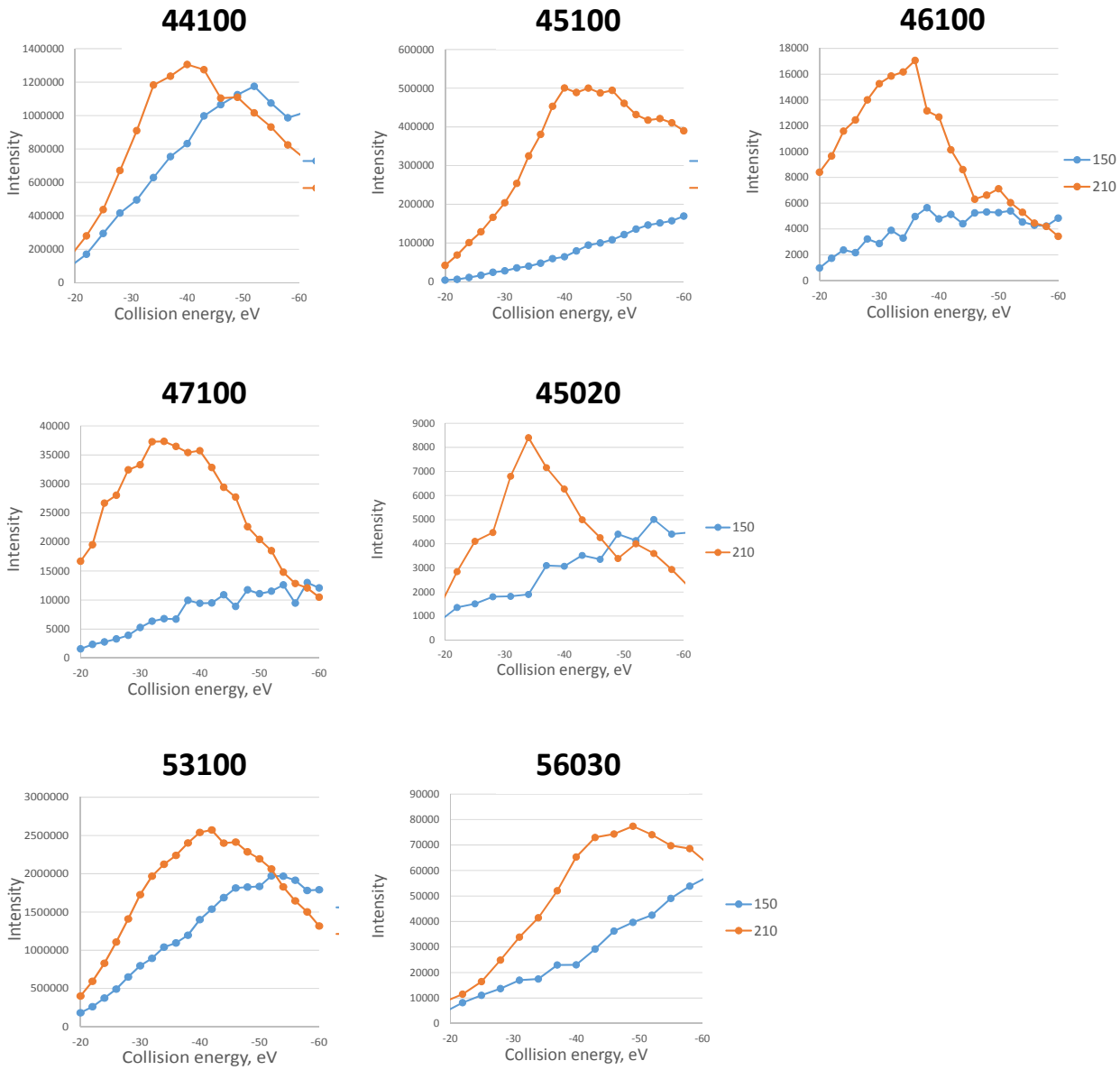

Figure S4. The energy-resolved product ion profiles of various peracetylated N-glycans. The CE-breakdown curves of representative per-acetylated N-glycan. *m/z* = 150.1 (HexNAc – $3H_2O$), *m/z* = 210.1 (HexNAc + Ac– $2H_2O$). Glycan composition is shown as Glycan ID, 5 digits correspond to: HexNAc, Hexose, Fucose, Neu5Ac, Neu5Gc.

Figure S5

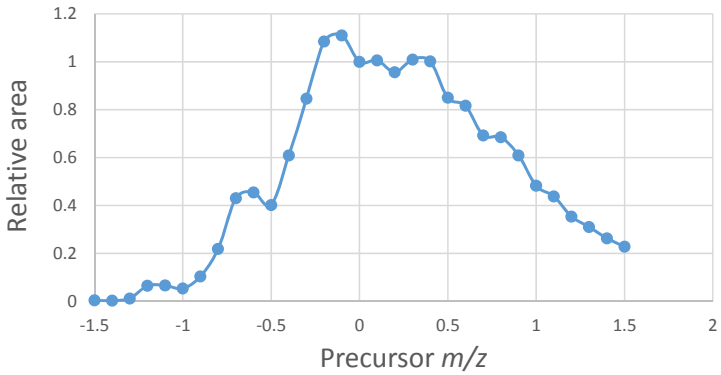

Precursor m/z	Relative area
-1.5	0.00415
-1.4	0.003165
-1.3	0.012028
-1.2	0.06529
-1.1	0.066058
-1	0.053882
-0.9	0.104634
-0.8	0.21938
-0.7	0.430509
-0.6	0.454726
-0.5	0.401971
-0.4	0.609732
-0.3	0.846112
-0.2	1.084771
-0.1	1.110006
0	1
0.1	1.006244
0.2	0.956488
0.3	1.009151
0.4	1.001702
0.5	0.850075
0.6	0.816349
0.7	0.693122
0.8	0.685507
0.9	0.609663
1	0.482873
1.1	0.438063
1.2	0.354103
1.3	0.310191
1.4	0.263247
1.5	0.228236

Figure S5. Identification of resolution of LCMS-8050 to evaluate the cross-talk. Peak area curve for Glycoform 43100 acquired at 0.1 Da intervals of precursor *m/z*.

Figure S6

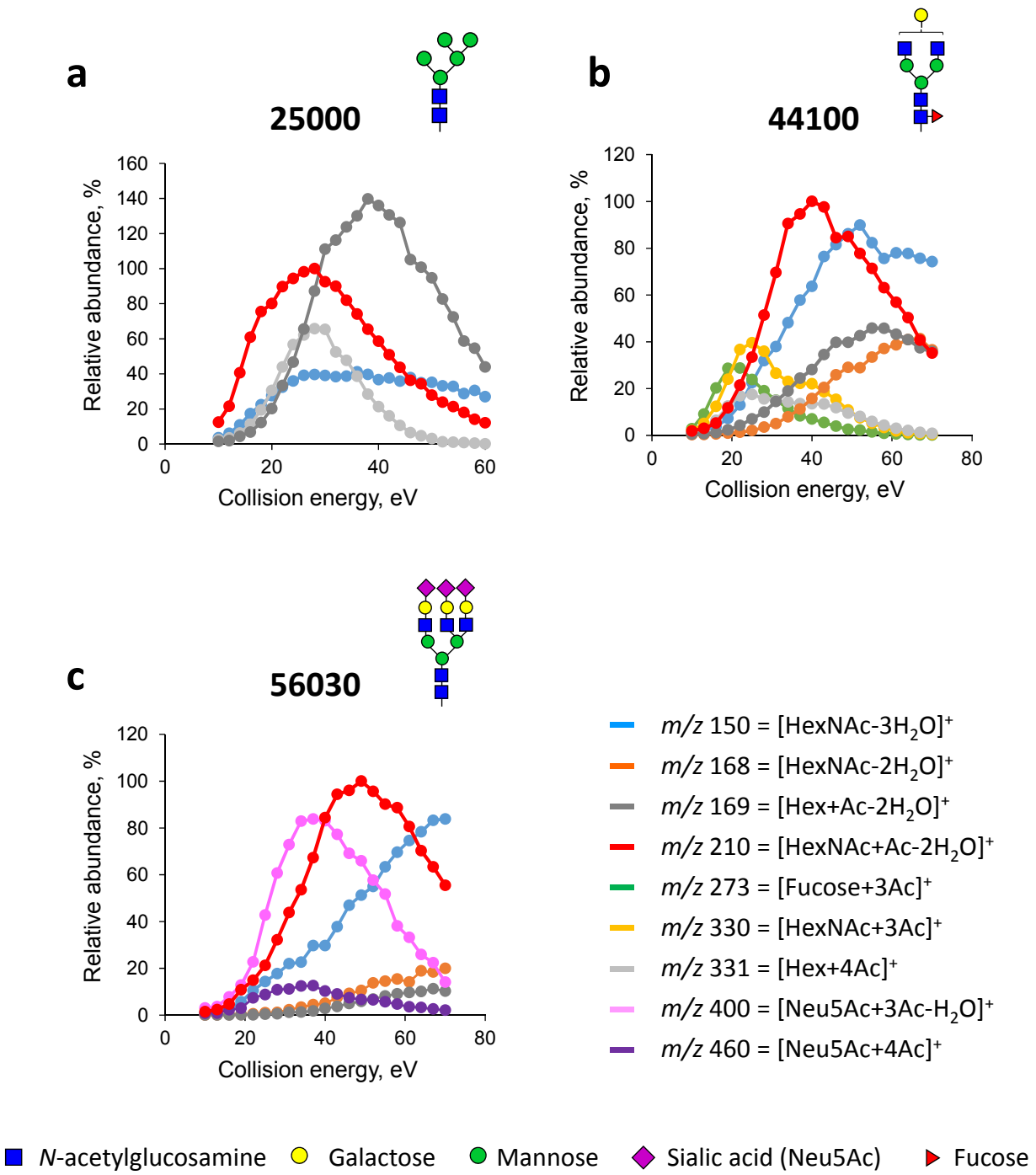

Figure S6. The energy-resolved product ion profiles of per-acetylated N-glycans. The Collision energy (CE)-breakdown curves of representative peracetylated N-glycan (Glycan ID: (a) 25000, (b) 44100, and (c) 56030). Glycan composition is shown as Glycan ID, 5 digits correspond to: HexNAc, Hexose, Fucose, Neu5Ac, Neu5Gc.

Figure S7

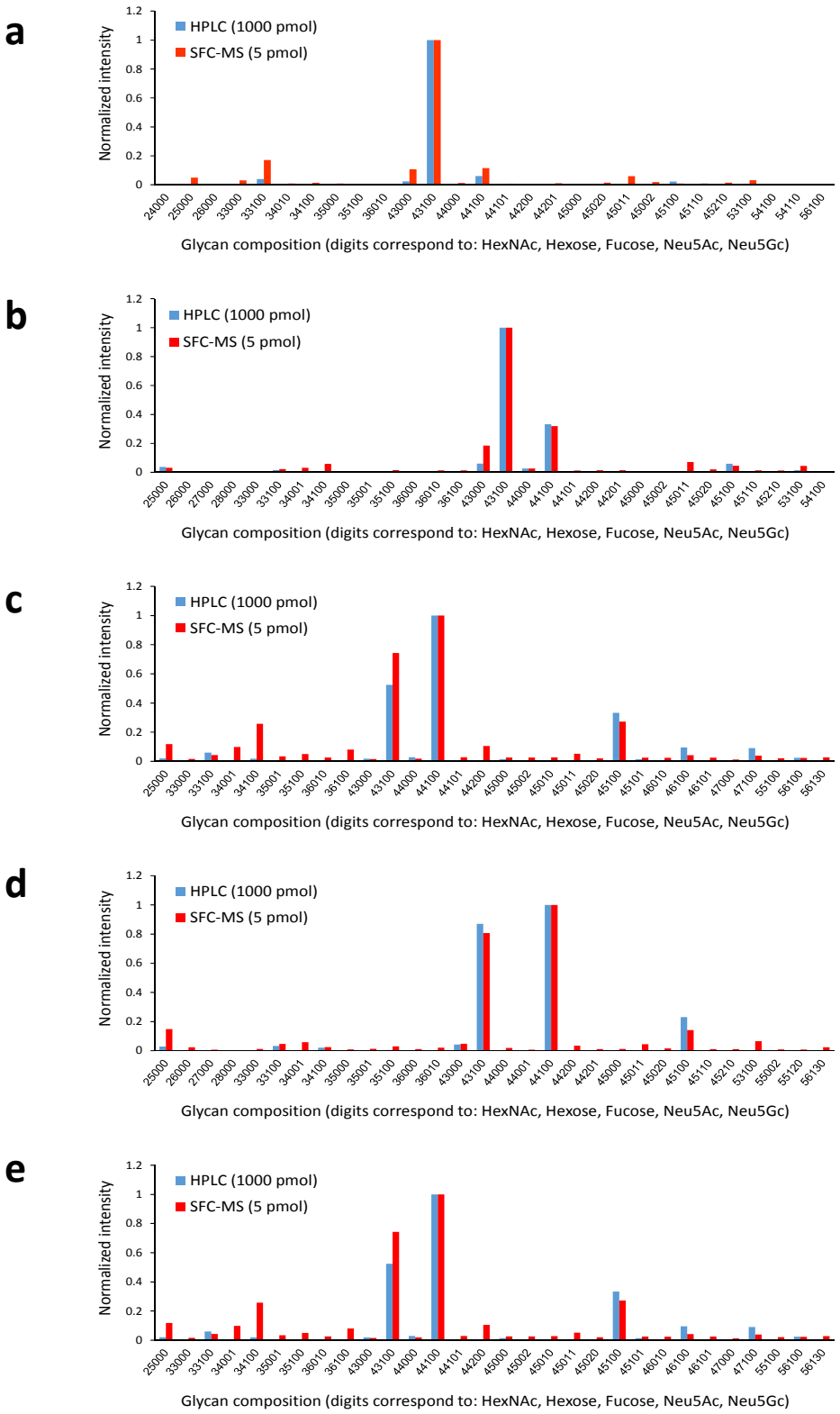

Figure S7. Comparison of therapeutic IgG N-glycan analysis of fluorescence HPLC and SFC-MS. Relative abundances observed for the top 30 N-glycans of (a) bevacizumab, (b) nivolumab, (c) ramucirumab, (d) rituximab, and (e) trastuzumab from HPLC analysis or SFC-MS analysis.

Figure S8

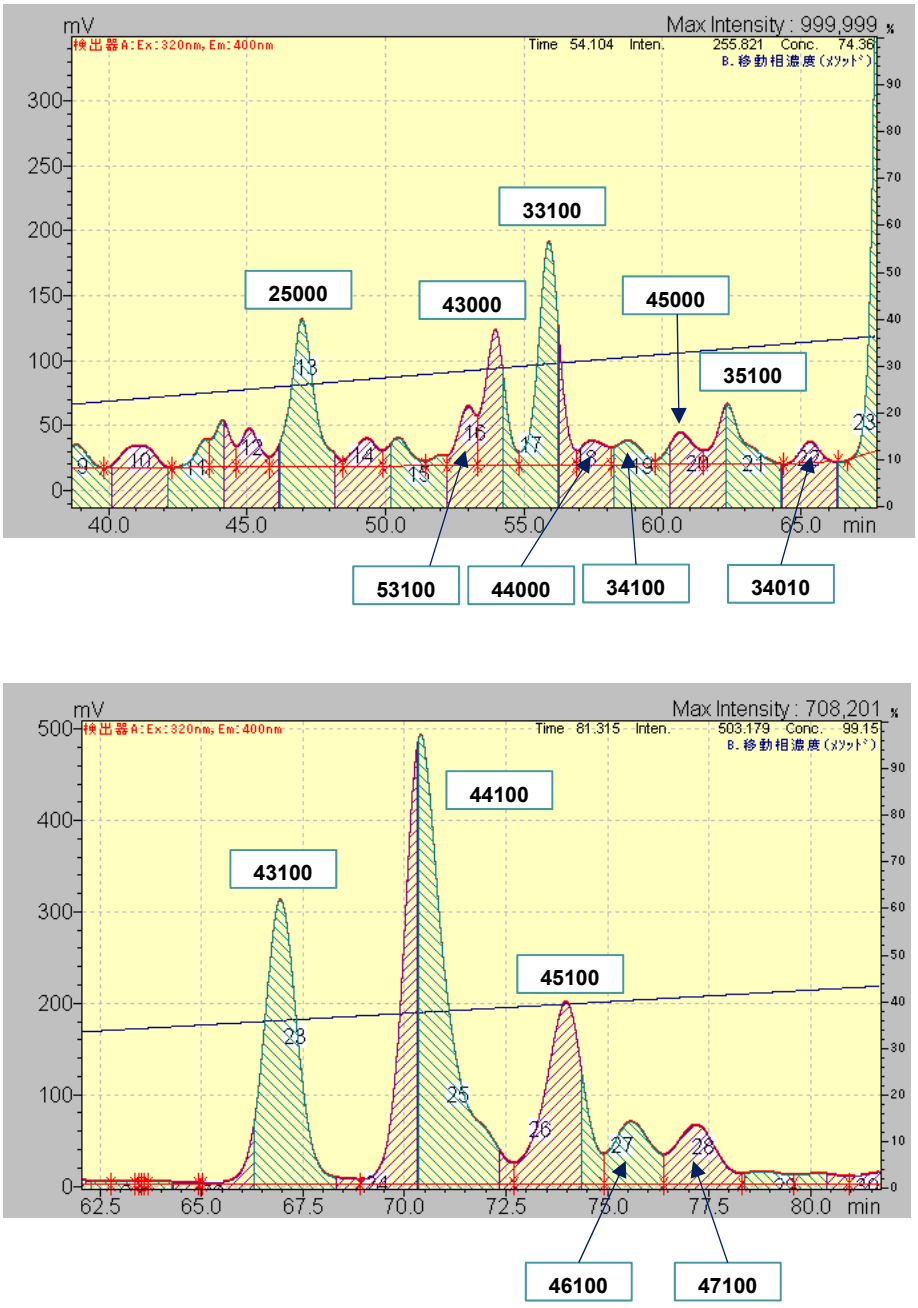

Figure S8. Elution profile of N-glycans from therapeutic antibodies analyzed by fluorescent HPLC. PA-derivatized N-glycans prepared from therapeutic antibodies were analyzed by reversed-phase HPLC.

Figure S9

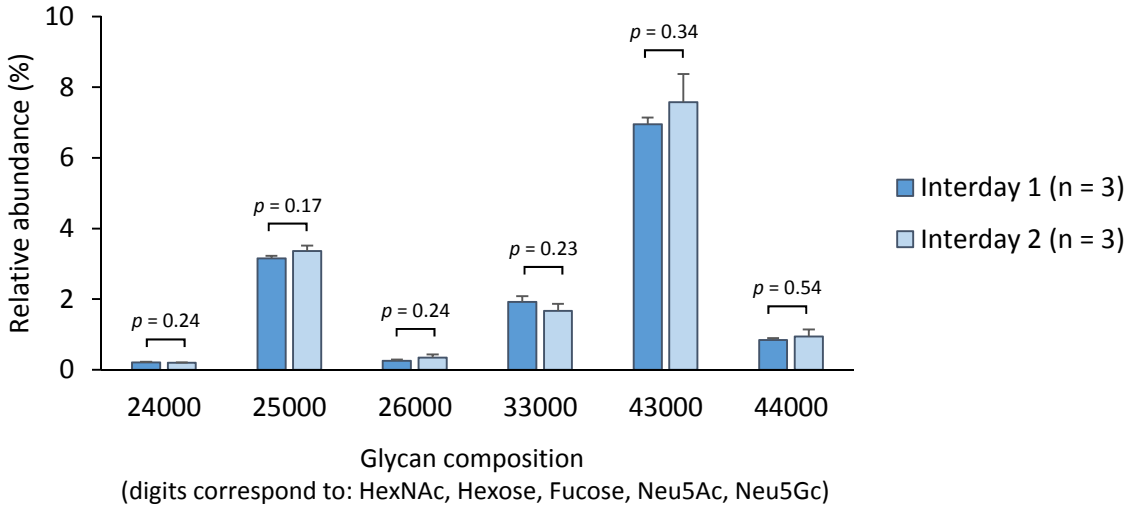

Figure S9. Inter- and intraday repeatability of low abundance glycan analysis by SFC-Erexim. The released N-glycans from bevacizumab were analyzed after acetylation. Error bars represent the standard deviation (intraday n = 3, independent technical experiments). The *p*-values were calculated by Student t-test.

Figure S10

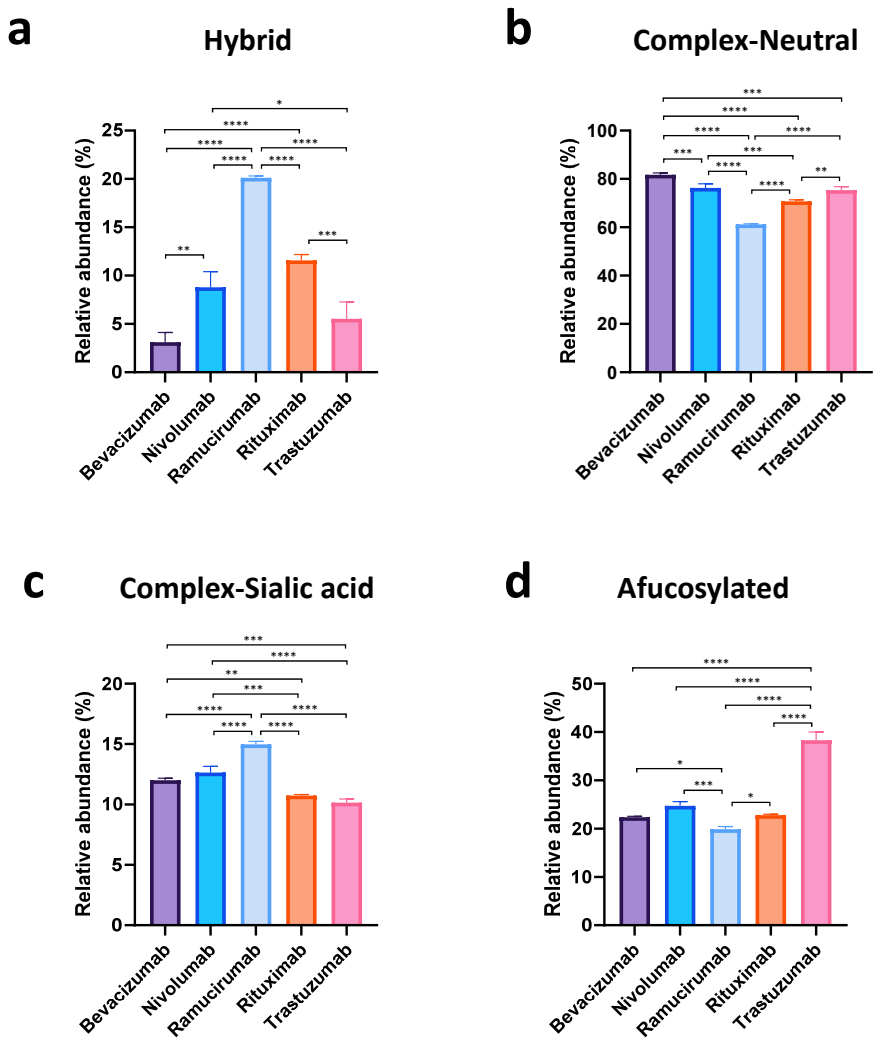

Figure S10. Comparison of N-glycans from five therapeutic antibodies. Relative abundances of (a) hybrid, (b) complex-neutral, (c) complex-sialic acid containing, and (d) afucosylated glycans of five therapeutic antibodies. Error bars represent the standard deviation (n = 3, independent technical experiments). The *p*-values were calculated by Tukey's multiple comparisons test. Only statistically significant differences are shown. $^{*}P < 0.05$, $^{**}P < 0.01$, $^{***}P < 0.001$, $^{****}P < 0.0001$.

Figure S11

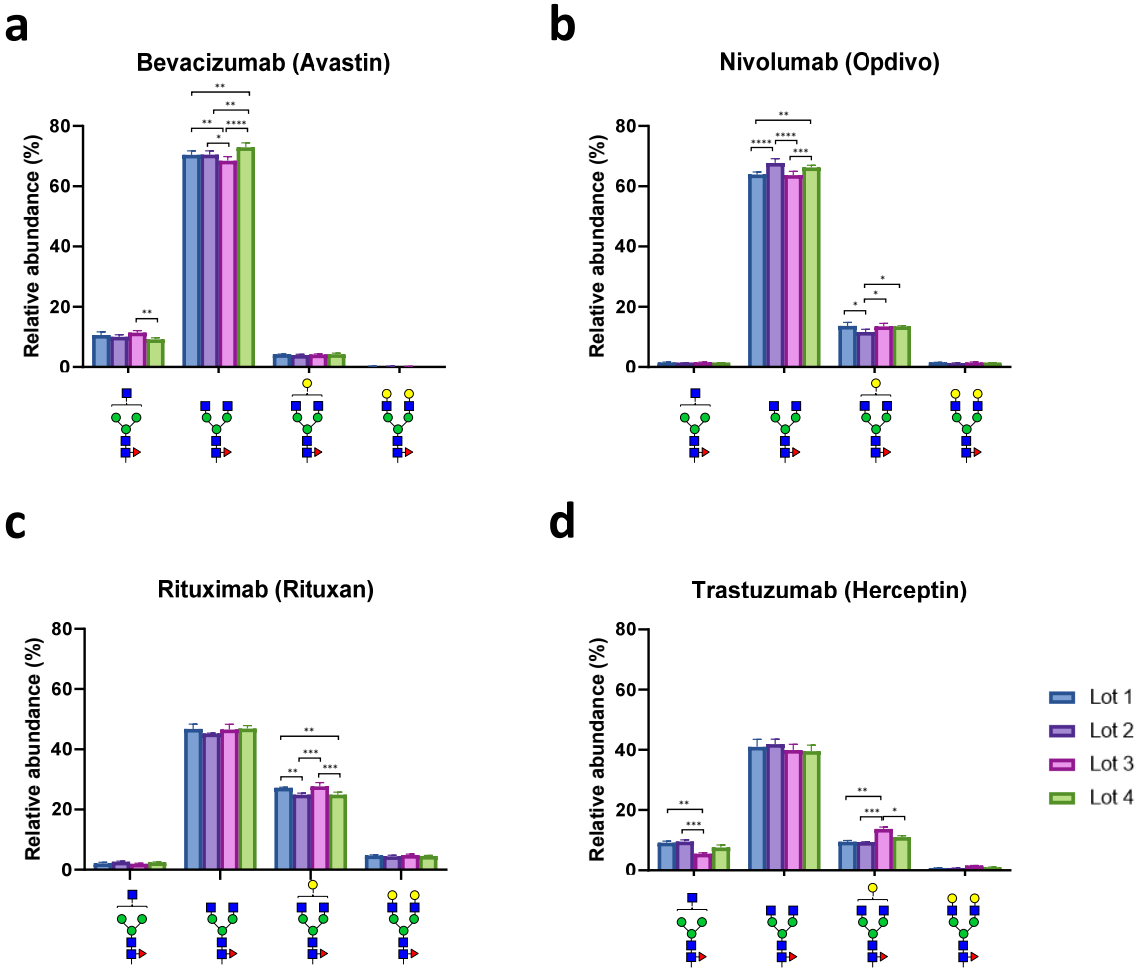

Figure S11. Evaluation of lot-to-lot heterogeneity for major fucosylated N-glycans. Relative abundances of Glycoform 33100, 43100, 44100, and 45100 of four lots of (a) bevacizumab, (b) nivolumab, (c) rituximab, and (d) trastzumab. Error bars represent the standard deviation (n = 3, independent technical experiments). The *p*-values were calculated by Tukey's multiple comparisons test. Only statistically significant differences are shown. $^{*}P < 0.05$, $^{**}P < 0.01$, $^{***}P < 0.001$, $^{****}P < 0.0001$.

Figure S12

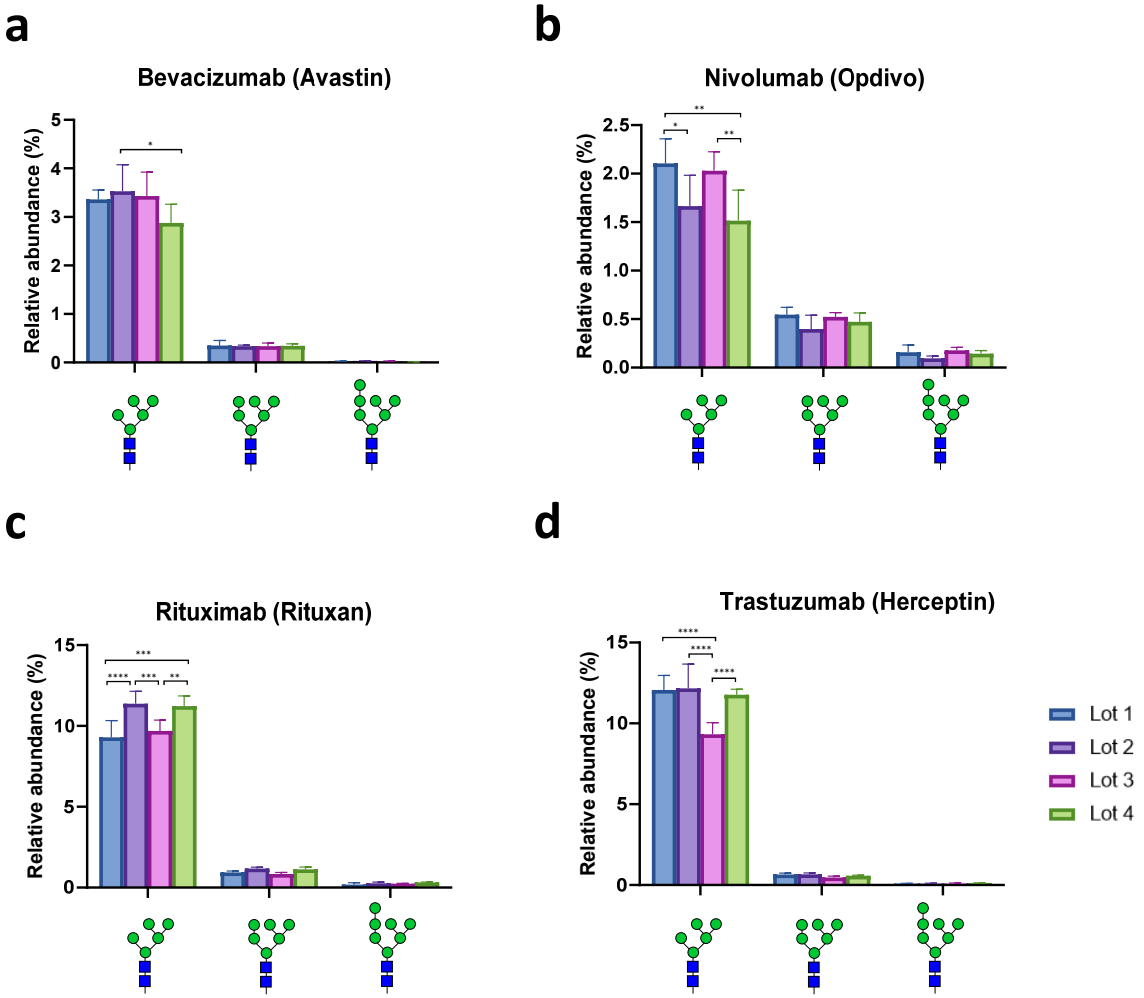

Figure S12. Evaluation of lot-to-lot heterogeneity for high mannose-type N-glycans. Relative abundances of Glycoform 25000, 26000, and 27000 of four lots of (a) bevacizumab, (b) nivolumab, (c) rituximab, and (d) trastzumab. Error bars represent the standard deviation (n = 3, independent technical experiments). The *p*-values were calculated by Tukey's multiple comparisons test. Only statistically significant differences are shown. $^{*}P < 0.05$, $^{**}P < 0.01$, $^{***}P < 0.001$, $^{****}P < 0.0001$.